

16 Tesla Block-Coil Dipole for Future Hadron Colliders*

Peter M. McIntyre and Weijun Shen

Department of Physics, Texas A&M University, College Station, TX 77843

Ronald M. Scanlan

Lawrence Berkeley Laboratory, Berkeley, CA 94720

Abstract—Several new concepts in magnetic design and coil fabrication are being incorporated into a design for an ultra-high field dipole magnet for future hadron colliders. The 16 Tesla block-coil dual dipole uses Nb₃Sn cable, a simple pancake coil construction, and face-loaded prestress geometry to achieve high magnetic efficiency and stable stress distribution at the limit of Nb₃Sn performance. A reverse-field end coil is used to cancel the concentration of field and stress at the coil ends and thereby eliminate the dipole ends as a limit to performance.

I. INTRODUCTION

The cost and performance of a hadron collider are largely determined by the field strength and field quality of its superconducting magnets. The dipole strength determines the circumference of the collider for a given beam energy; the quadrupole strength determines the low-beta squeeze of the beams at the collision point; the dipole field quality determines the sustainable luminosity and the complexity of correction elements required in the collider lattice. As the high energy physics community assesses its options for future hadron colliders, magnet technology will set the limits for cost, performance, and siting.

In conventional dipole design^[1], a $\cos \theta$ coil configuration is supported within a non-magnetic collar within a steel yoke. In a previous paper^[2], we reported a design for a 16 Tesla block-coil dipole, consisting of a rectangular coil configuration closely coupled to a steel yoke. It offers improved magnetic efficiency, stable confinement of the Lorentz forces, and simple coil fabrication. The block-coil dipole is being developed in a collaboration between Lawrence Berkeley Laboratory and Texas A&M University. In this paper we report progress in the design and preparations for construction of short model magnets.

Figure 1 shows the overall magnet design and coil configuration for a 16 Tesla dual dipole utilizing Nb₃Sn Rutherford cable. Table I presents its main parameters. All coil elements are arranged in flat pancake coils, in which the cable is oriented flat to the direction of Lorentz forces. The coil is divided into three segments to facilitate grading of the conductor with $j_c(B)$ and optimization of field quality. This coil configuration provides a stiff modulus for preload, a simple procedure for coil winding and positioning, and a compact current geometry for minimum amp-turns.

*This work was supported in part by DOE grant DE-FG02-91ER40613.

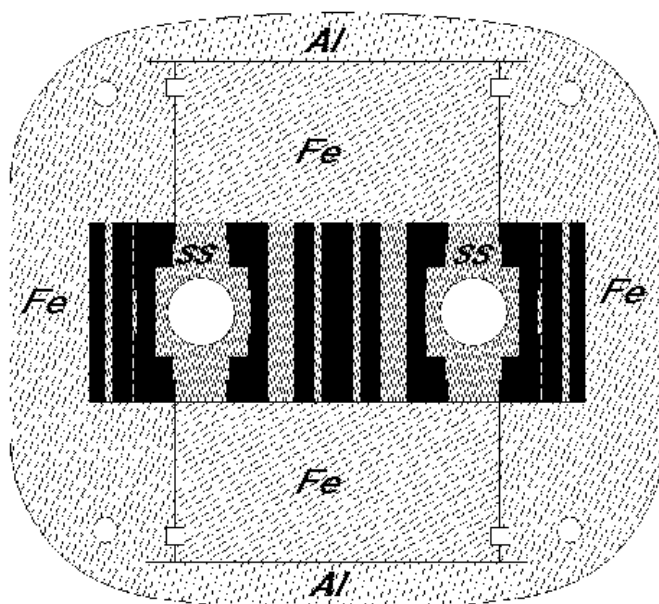


Figure 1. Block-coil dual dipole: coil configuration and preload strategy.

TABLE I
PARAMETERS OF BLOCK-COIL DUAL DIPOLE

Peak Field	16	Tesla
Beam tube aperture radius	2.5	cm
Maximum current	9,300	Amperes
Operating temperature	4.2	°K
Stored energy	4.36	MJ/m
Inductance	101	mH/m
Total turns	580	
Lorentz stress	170	MPa
Maximum j_{Cu} during quench	1,100	A/cm ²
Overall cold mass: radius	25	cm
mass	1,260	kg/m
Fringe field at cryostat surface	.1	Tesla

I. FIELD DESIGN

Figure 2 shows the calculated field distribution in the magnet at 16 Tesla excitation. We have designed the coil geometry to produce collider-quality field uniformity (all multipoles $b_n < 10^{-4}$ cm⁻ⁿ) at full excitation B_0 , using equal current in all three coils. The innermost coil segment approximates a $\cos \theta$ distribution; the outer two segments are planar current sheets; the gaps between coil segments are made asymmetric to compensate the asymmetry produced by the opposite dipole. We can produce quality field at all in-

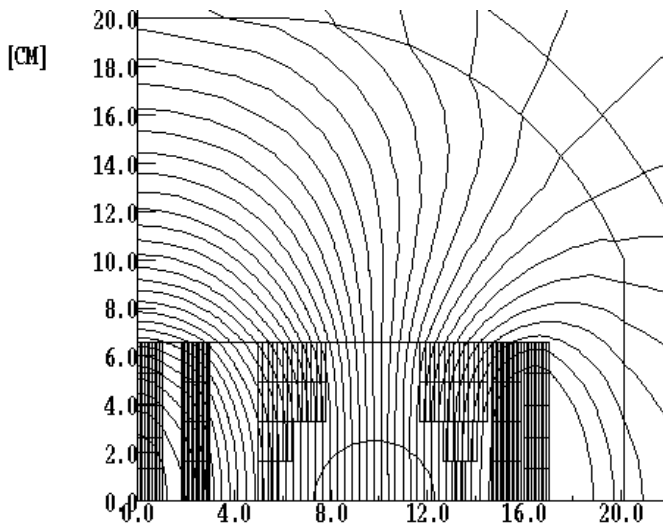


Figure 2. Calculated field distribution in one quadrant of block-coil dipole. intermediate field strengths by current programming the three coil segments. Figure 3 shows the current program as a function of excitation over a 20:1 dynamic range.

Persistent-current multipoles and AC losses.

The planar steel boundary above and below each beam tube serves to suppress the multipole fields induced by magnetization currents in the superconducting strands as the magnet is ramped from injection to full field and back. Figure 4 shows the calculated persistent current sextupole in the block dipole. The hysteresis at injection is ten times smaller than that in a $\cos \theta$ dipole with similar filament size.

Because the cable elements are turned edge-on to the magnetic flux in the coil region, AC losses should also be ~ 10 times smaller than in $\cos \theta$ dipoles.

II. COIL STABILIZATION

Reverse-Field End Stabilization

In any superconducting dipole, the coil ends are one of the most challenging limits for high-field stability. The fields are greatest at the ends; the forces are greatest in the ends and are difficult to preload around there; the conductor is somewhat degraded by bending there so that $j_c(B)$ is less there than in the body of the coil. All three effects make the end the “weak sister” of the dipole - the first location for failure.

We have conceived a means to eliminate this problem, by bracketing the end region with an array of reverse-field coils which cancel $\sim 30\%$ of the field at the location of the end turns of the dipole coil. The reverse-field coil arrangement is shown in Figure 5. The reverse coils are tilted so that their field cancels part of the primary field at the coil ends but does not produce significant field on the body portion of the main coil. The reverse coils of course experience large forces and fields. They are supported within an end steel structure and are designed with ample margin ($j/j_c \sim 0.5$) and stability ($Cu:SC \sim 2$).

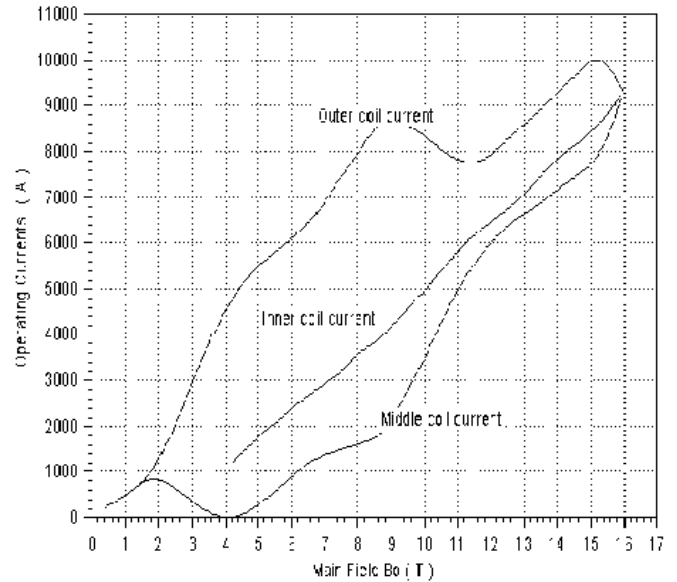


Figure 3. Current programming of the three coil segments.

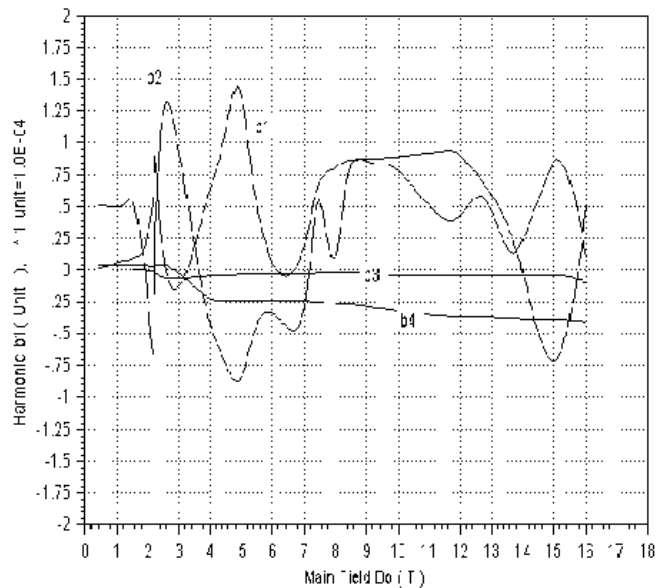


Figure 4. Residual multipoles including magnetization during ramping (PE2D).

The essential novelty of the reverse coil is to displace the problem of end fields and stresses to a compact coil which is only provided at the ends. The body coil must be driven to its practical limit, $j/j_c \rightarrow 90\%$, because most of the collider circumference is filled with dipole body and the conductor dominates the magnet cost. The ends, on the other hand, occupy only a few % of the magnet length, and the additional conductor to provide stable reverse coils is insignificant in the overall conductor budget.

Quench protection.

With a stored energy of 2.2 MJ/m in each dipole, quench protection is a critical consideration for reliable magnet operation. The parameter which is of greatest importance in quench dynamics is the maximum current density j_{Cu} which would appear in the copper stabilizer of the cable

during a quench. If $j_{Cu} < 1,100 \text{ A/cm}^2$, active quench protection using appropriate arrangements of clamp diodes, limiting resistors, and pulsed heaters can typically be used to safely distribute a quench so that a magnet consumes its stored energy without overheating at any location. We have adopted this limit in the block-coil dipole. Preliminary simulations have been made of quench propagation in the block-coil dipole using a heater/diode/resistor protection network. During a quench the current decays with a time constant $\sim 0.2 \text{ s}$, the maximum coil temperature is $\sim 430^\circ\text{K}$, and the maximum voltage is $\sim 1,300 \text{ V}$.

III. FABRICATION ISSUES

Coil preload strategy.

The rectangular coil package and rectangular steel flux return presents a particularly simple means for delivering a uniform preload to the entire coil. The steel flux return is divided along the in/out bifurcation of the return flux. The blocks are assembled with an aluminum bar to provide a gap at room temperature. The gap closes as the magnet is cooled down, and the bar dimensions are chosen so that the gap closes at 4.2°K and compensates the loss of compression which would otherwise occur from the differential contraction of the coil and the steel. The steel assembly is preloaded by wrapping a high-strength steel banding around the overall assembly. Preliminary stress analysis shows that this approach can be used to provide a uniform laminar horizontal prestress of 200 MPa to the coil while containing vertical coil dimensions.

E. Coil fabrication.

The coils of Nb_3Sn Rutherford cable must be fabricated using the wind-and-react method. We are developing a flat/bend winding procedure to simplify and improve coil fabrication. All coil elements are wound as flat racetrack coils. Adjacent pairs of coil elements are wound from the inside out from a single length of cable, so that all leads emerge on the outside ends of the coil package.

The racetrack coil is an ideal geometry in which to eliminate the flexure and handling of the coil and its insulation during fabrication. It presents a problem, however, for the coil elements which flank each beam tube: they must be bent up and over the beam tube at the ends. We have developed a procedure whereby these coils are also wound as flat racetracks, and then bent at the ends in a simple fixture so that each clears the beam tube. The final end configuration can be preloaded using precast spacer/tensor elements.

Inorganic cable insulation matrix.

Even with the elimination of stress concentrations, the Lorentz stress at 16 Tesla is immense - 170 MPa. Impregnation of the cable elements within the coil is essential, both to prevent stress concentrations where strands overlap in the cable and to provide electrical insulation during quench.

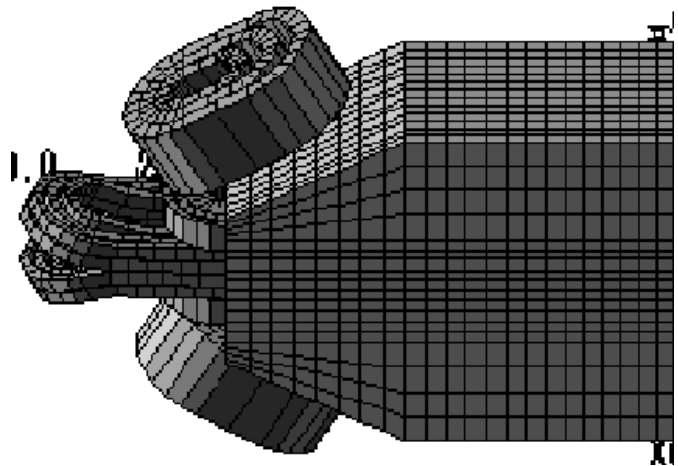


Figure 5. Reverse-field stabilization of the coil ends (TOSCA simulation)

Conventionally Nb_3Sn coils are impregnated with organic polymers after reaction bake. The poor heat conductivity of such materials limits heat transport through the thick coil package required for a 16 Tesla dipole. Both beam losses and synchrotron radiation produce substantial heat loads to the inner coil elements. Poor heat transport also compromises stability against micro-quenches.

We are endeavoring to overcome these problems by using an “inorganic B-stage” process which would provide inter-strand mechanical support and electrical insulation but preserve an open porosity for liquid He to permeate the coil package. The approach is motivated by work at Ceramphysics and Westinghouse^[3], Tanaka *et al.*^[4], and Shultz and Reed^[5]. A glass/ceramic mixture is mixed with a silicone binder to coat the strands of each cable element in the green state (before winding). The treated cable is sheathed in an E-glass wrap to provide inter-cable isolation. The glass component is chosen to have a vitrification temperature near the high end of the reaction bake cycle. It flows to uniformly fill the inter-strand space. The ceramic component provides powder reinforcement of the glass and local heat capacity at 4°K . After the Nb_3Sn reaction bake, the insulation provides mechanical support and electrical insulation to each cable element, but leaves open for helium percolation. Liquid helium can permeate this space, bathe the coil, and provide local enthalpy to stabilize against microquenches.

It is a pleasure to acknowledge the ongoing help of S. Caspi, F. Clark, W. Kroenke, A. McInturff, N. Munshi, H. van Oort, W. Sampson, and C. Taylor.

REFERENCES

- [1] R. Perin, “Status of the LHC programme and magnet development”, Proc. Appl. Superconductivity Conf., Boston, MA, October 14-17, 1994.
- [2] D. Dell’Orco *et al.*, “Fabrication and preliminary test results for a Nb_3Sn dipole magnet”, *ibid.*
- [3] P. McIntyre, R. Scanlan, and W. Shen, “Ultra-high-field magnets for future hadron colliders”. *ibid.*
- [4] W.N. Lawless and C.F. Clark, J. Appl. Phys. **64**, p.2729 (1988).
- [5] K.H. Tanaka *et al.*, IEEE Trans. Magnetics **30**, p.2511 (1994).
- [6] J. Schultz and R.P. Reed, “Inorganic and hybrid insulation materials for ITER”, MIT Plasma Fusion Center (1993).